IET Nanobiotechnology

Research Article

IET Journals
The Institution of Engineering and Technology

Synthesis and comparative assessment of antiradical activity, toxicity, and biodistribution of κ-carrageenan-capped selenium nanoparticles of different size: in vivo and in vitro study

ISSN 1751-8741
Received on 27th January 2020
Revised 3rd May 2020
Accepted on 28th May 2020
E-First on 14th July 2020
doi: 10.1049/iet-nbt.2020.0023
www.ietdl.org

Marina Lesnichaya[1] ✉, Roman Shendrik[2], Evgeniy Titov[3], Boris Sukhov[1]

[1]A. E. Favorsky Irkutsk Institute of Chemistry, Siberian Branch, Russian Academy of Sciences, 1 Favorsky Str., 664033, Irkutsk, Russia
[2]A.P. Vinogradov Institute of Geochemistry, Siberian Branch, Russian Academy of Sciences, 1a, Favorsky Str., 664033, Irkutsk, Russia
[3]East-Siberian Institute of Medical and Ecological Research, Bldg. 3, Microdistric 12a, P.O. Box 1170, 665827, Angarsk, Russia
✉ *E-mail: mlesnichaya@mail.ru*

Abstract: In the present study, water-soluble hybrid selenium-containing nanocomposites have been synthesised via soft oxidation of selenide-anions, preliminarily generated from elemental bulk-selenium in the base-reduction system 'N_2H_4–NaOH'. The nanocomposites obtained consist of Se^0NPs (4.6–24.5 nm) stabilised by κ-carrageenan biocompatible polysaccharide. The structure of these composite nanomaterials has been proven using complementary physical–chemical methods: X-ray diffraction analysis, transmission electron microscopy, optical spectroscopy, and dynamic light scattering. Optical ranges of 'emission/excitation' of aqueous solutions of nanocomposites with Se^0NPs of different sizes are established and the most important parameters of their luminescence are determined. For the obtained nanocomposites, the expressed antiradical activity against free radicals 2,2-diphenyl-1-picrylhydrazyl and 2,2′-azino-bis(3-ethylbenzothiazoline-6-sulphonic acid has been found, the value of which depends on the size of selenium nanoparticles. It is experimentally revealed that all obtained nanocomposites are low toxic (LD_{50} >2000 mg/kg). It is also found that small selenium nanoparticles (6.8 nm), in contrast to larger nanoparticles (24.5 nm), are accumulated in organisms to significantly increase the level of selenium in the liver, kidneys, and brain (in lesser amounts) of rats.

1 Introduction

Selenium is one of the most important microelements [1]. It is met in active centres of selenium-containing enzymes involved in the metabolism of nucleic acids, lipids, and hormones. Selenium also performs the function of antioxidant protection of cells from a number of aggressive free radicals that are constantly formed in the body due to both natural metabolic processes and in elevated amounts in the case of cell interaction with pathogenic agents (viruses, microbes, toxins, inflammatory factors, and tumour growth and decay factors) [2, 3]. The animal organism is extremely sensitive to disorders of selenium homeostasis. Selenium deficiency leads to such diseases as exudative diathesis, liver necrosis, Keshan and Kashin-Bek diseases [4]. Therefore, the prevention of selenium deficiency represents an urgent challenge. Among the popular compounds used to compensate selenium deficiency in the organism are sodium selenite and selenate, as well as selenomethionine [5]. However, the high toxicity of inorganic forms of selenium and extremely high reactivity of organic forms of selenium, leading to cell damage, limit their biological applications and stimulate the search for less toxic sources of selenium. As an alternative, it is possible to employ nanoparticles of the elemental selenium (Se^0NPs), which have low toxicity and possess high biological activity, in particular, very important antioxidant action [6–8]. In addition, small-sized Se^0NPs exhibit luminescence in the spectral region of the 'window of tissue transparency'. They can be used as imaging agents for cancer diagnostics [9, 10]. Good water solubility, bioavailability, and stability of Se^0NPs, which depend upon the synthesis conditions, are the key factors for biomedicine application of these compounds. Be the moment, numerous studies have convincingly demonstrated the antioxidant effects of Se^0NPs on various free radicals [11, 12]. However, known and most common methods for their synthesis include either chemical reduction of inorganic compounds of selenium (Na_2SeO_3, SeO_2, H_2SeO_3 etc.) by active reducers (sodium borohydride, hydrazine hydrate etc.) or various plant extracts and products of microbial metabolism [13–16] or physical action using powerful energy sources (laser, radiation reduction etc.) [17, 18]. The main disadvantages of these methods are the employment of the special expensive equipment (in the case of physical synthetic methods), as well as various reducing agents. In the latter case, unreacted residues and various by-products contaminate the target compounds, thus requiring sophisticated purification of the resulting nanomaterials. All of the above determines the high cost and prolonged duration of Se^0NPs synthesis by these methods, as well as the negative effect of products obtained after purification of the target material on the environment. In addition, these disadvantages may limit the biomedical application of these valuable nanomaterials. This problem could be addressed by the synthesis of Se^0NPs directly from the elemental bulk selenium, which is an inexpensive and available chemical precursor, and also using natural water-soluble sulphated polysaccharide κ-carrageenan (κ-CG). Previously, κ-CG has shown itself as an effective stabiliser of the inorganic nanoparticles (Ag, Au, CdSe, and NH_4MgPO_4) [19–22]. At the same time, κ-CG is a renewable natural raw material widely employed in the food and pharmaceutical industries [23]. It possesses various biological activities (anticoagulant [24], antiviral [25], immunomodulatory [26] etc.) [27]. The incorporation of the Se^0NPs in the κ-CG polysaccharide matrix can lead to the formation of the hybrid nanocomposites, which combine the properties of their inorganic component (optical and antioxidant properties) and those of κ-CG. Moreover, valuable biological and optical properties of these nanocomposites can be directly controlled by the size characteristics of the obtained Se^0NPs.

This study is focused on the synthesis of selenium nanoparticles from elemental bulk-selenium powder using κ-CG as a capped agent. Also, the composition and structure of the obtained nanomaterials are characterised in detail. Furthermore, the relationship between the size of the selenium nanoparticles and their properties, including the effect on a living organism, biodistribution, toxicity, and antiradical properties has been established.

2 Experimental

2.1 Materials

In this work, we used κ-CG (M_W=1100 kDa) from CP Kelco (USA), powder selenium, sodium hydroxide, hydrazine-hydrate (64%), and ethyl alcohol (96%) were purchased from Vecton (Russia). 2,2′-Azino-bis(3-ethylbenzothiazoline-6-sulphonic acid) (ABTS) and 2,2-diphenyl-1-picrylhydrazyl (DPPH) were purchased from Sigma-Aldrich. All chemicals were used as received without additional purification

2.2 Synthesis of Se^0NPs-containing nanocomposites

Synthesis was carried out in accordance with the previously described technique [28] with minor experimental changes that allowed to obtain a wider range of nanocomposites with different content of Se^0NPs, as well as to overcome diffusion difficulties in the migration of selenium atoms in the process of nucleation and growth of nanoparticles due to the aggregation and gel formation of κ-CG macromolecules in the presence of potassium ions. Briefly, in a three-necked flask equipped with a reflux condenser and a thermometer, 1 g NaOH and 0.5 ml $N_2H_4 \cdot H_2O$ were placed under constant stirring, then the temperature of this reaction medium was brought to 70°C and 0.98 g of elemental bulk-selenium was added under an argon atmosphere. The synthesis time was 30 min. The formation of highly reactive Se^{2-}anions was accompanied by the appearance of a characteristic red-maroon stain and complete dissolution of selenium. Next, an aliquot of the obtained reaction mixture containing Se^{2-}-anions (V 5–25 µl) was added to the previously obtained κ-CG solution (1.0 g κ-CG in 80 ml water) and stirred at room temperature for 20 min. The isolation of the target nanocomposites and their purification from impurities was performed by precipitation with a four-fold excess of EtOH, followed by repeated washing with ethanol and drying in air at room temperature. The content of Se^0 in the obtained nanocomposites was 0.3, 0.6, 1.0, and 1.5% by mass. Yield 80–96%.

In addition, for a comparative study of the biological effect of selenium nanoparticles of different sizes, we obtained a nanocomposite sample containing selenium particles with an average size of 24.5 nm. It was synthesised using a similar procedure for the preparation of other nanocomposites, with the only exception that the volume of an aliquot of the reaction medium containing Se^{2-} ions was 50 µl. The content of selenium was 3.0% and the yield was 94%.

2.3 Characterisation and measurements

2.3.1 Infrared spectroscopy (IR) of native κ-CG and Se0NPs-containing nanocomposites: IR spectra were recorded by using a Fourier transform-infrared (RAM II) Bruker Vertex 70 spectrometer in potassium bromide pellets in the range of 4000–400 cm^{-1}.

2.3.2 X-ray diffraction (XRD) analysis: XRD study was carried out on a Bruker D8 ADVANCE X-ray diffractometer with Cu Kα radiation mode locked coupled. The exposure time was 1 s for the phase analysis, and 3 s for the cell parameters and coherent lengths.

2.3.3 Transmission electron microscopy (TEM): TEM measurements were performed on a Leo 906 E microscope operated at an accelerating voltage of 120 kV. The size distribution of nanoparticles was determined by the statistical processing of TEM microphotographs.

2.3.4 Elemental analysis: The elemental composition was determined with a Thermo Scientific Flash 2000 CHNS analyser and by X-ray energy dispersive microanalysis with a Hitachi TM 3000 scanning electron microscope equipped with a SDD XFlash 430-4 X-ray detector. The sulphatation degree of κ-CG and its nanocomposites was determined by elemental analysis (according to the ratio of sulphur to carbon, hydrogen, and oxygen contents). Elemental analysis of κ-CG: C (33.1%), H (6.1%), S (6.8%), Na (3.36%), and K (3.6%).

2.3.5 Optical and luminescent spectroscopy: All optical spectral measurements were performed with a water solution of Se^0NPs in a quartz cuvette. The optical absorption spectra were obtained on a Perkin-Elmer Lambda 950 ultraviolet/visible/near-infrared spectrophotometer. Photoluminescence (PL) and PL excitation spectra of water solution Se^0NPs were obtained with a Perkin Elmer LS-55 instrument.

2.3.6 Dynamic light scattering analysis (DLS) and measurement of ζ-potential: DLS measurements were performed using a Photocore Compact-Z equipment at 23±0.1°C. A software package DynaLS v2.0 (ALANGO) was used to calculate the correlation time distributions. Scattering angle was 90°, laser 654 nm, and power 20 mV. The solutions were prepared at least 10 h before the measurements. To dispose of dust, the scattering cells were rinsed with benzene, vacuumised, and filled with dust-free air. Taking into account the polyelectrolyte character of κ-CG, its nanocomposites were studied in water-salt solutions 0.1 M NaCl. Then the solutions were filtered through a cellulose acetate filter with 0.45 µm pores.

The polyelectrolyte velocity ν under external electric field E was measured. The electrophoretic mobility $\mu E = \nu/E$ was converted into the ζ-potential (the potential of electrical double-layer at the surface of hydrodynamic shear) by the Smoluchovsky equation $\mu E = \varepsilon\varepsilon o\zeta/\eta s$, where ε and εo are the dielectric permittivities of the solvent and vacuum, respectively. Each measurement was performed three times, the results were averaged.

2.4 Estimation of antioxidant activity

2.4.1 DPPH radical-scavenging activity: The scavenging activity of nanocomposites Se^0/κ-CG and native κ-CG against DPPH radical was measured by Yamaguchi's method [29] and according to the recommendation of Molyneux [30] with slight modifications. Briefly, 2.5 ml of the sample solution at different concentrations (0.25–10 mg/ml) was mixed with 2.5 ml of 1.26×10^{-4} mol/l DPPH solution in the phosphate buffer (pH 5.5). The mixture was shaken vigorously and incubated for 30 min at 33°C in the dark. Finally, the absorbance was measured at 515 nm in 1 cm quartz cuvette. Ascorbic acid was used as a reference. The DPPH radical inhibition (%) was calculated by the following equation:

$$\text{DPPH scavenging ability}\,(\%) = \left[1 - \left(\frac{A_a - A_b}{A_c}\right)\right] \times 100\% \qquad (1)$$

where A_a is the absorbance of the sample mixed with DPPH solution, A_b is the absorbance of the sample without DPPH solution, and A_c is the absorbance of DPPH solution without the sample as a blank control.

2.4.2 ABTS radical-scavenging activity: The scavenging activity of nanocomposites Se^0/κ-CG and native κ-CG against ABTS cation-radical was measured as described by Cai *et al.* [31] and according to the recommendation of Re *et al.* [32] and Erel [33] with some modifications. Generally, 7.34 mmol/l of ABTS solution reacted with 20 mmol/l of potassium persulphate to obtain

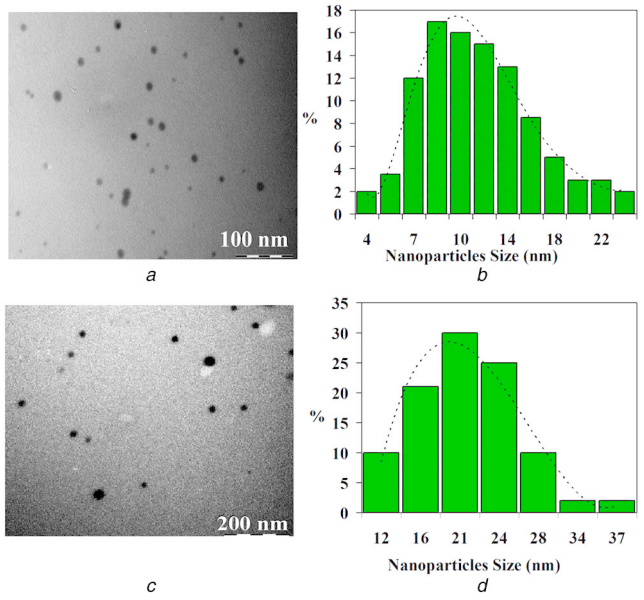

Fig. 1 *TEM images of nanocomposites Se^0/κ-CG containing* ***(a)*** 1.5% Se, ***(c)*** 3.0% Se, ***(b, d)*** Diagrams of their size distribution

ABTS cation-radical ($ABTS^{\bullet+}$). The mixture was kept in the dark for 12–16 h at room temperature, then the $ABTS^{\bullet+}$ solution was diluted to a stable absorbance of 0.70 ± 0.01 at 734 nm. Next, 1.4 ml of the sample solution at various concentrations (0.25–3 mg/ml) was mixed with 0.7 ml of the diluted $ABTS^{\bullet+}$ solution. After reaction for 6 min at 30°C, the absorbance was measured at 734 nm in 1 cm quartz cuvette. Ascorbic acid was used as a reference. The ABTS cation-radical inhibition (%) was calculated by the following equation:

$$\text{ABTS scavenging ability}\,(\%) = \left[1 - \left(\frac{A_a - A_b}{A_c}\right)\right] \times 100\% \qquad (2)$$

where A_a is the absorbance of the sample mixed with ABTS solution, A_b is the absorbance of the sample without ABTS solution, and A_c is the absorbance of ABTS solution without the sample as a blank control.

2.5 In vivo investigation of biological effects and biodistribution of selenium nanoparticles of different size

The studies were performed on 40 outbred white male rats with a weight of 180–200 g. The animals were divided into four groups containing 10 animals each. Animals of experimental groups were given (per-oral) 500 μg/kg of body weight for 10 days. The animals of the first (control) group were administered with distilled water. The animals of the second group were administered with nanocomposite Se/κ-CG with an average size of particles 6.8 nm. The animals of the third group received the nanocomposite Se/κ-CG with the average size of particles 24.5. The fourth group of animals was given pure κ-CG. After exposure, the animals were decapitated. Macroscopic analysis of the experimental animals' organism and microscopic analysis of the state of brain tissue, liver, and kidneys of the experimental animals were carried out. Analysis of selenium content in these organs was also performed for groups treated with selenium nanocomposite. Selenium content in biological tissues was determined by atomic absorption spectroscopy.

2.6 Investigation of toxicity of selenium nanocomposites

General toxicity was studied by determining the mean lethal dose (LD_{50}) of the nanocomposite, which was injected intragastrically by an atraumatic catheter at doses of 2000 mg/kg diluted in distilled water (0.5 ml) to 20 white mice males (10 mice in each group for the nanocomposites with a selenium particle size of 6.8 and 24.5 nm) using the Litchfield—Wilcoxon method. Animals were fed 3 h after administration of the compound and were observed for 14 days. The general condition (appearance, skin condition, hyper salivation, and death) and changes in behaviour were assessed. The control group received equivalent volumes of distilled water. At the end of the observation period, an autopsy of animals was performed to macroscopically examine the state of the internal organs of animals. The hazard category was determined according to GOST 12.1.007–76 'Noxious substances, classification and general safety requirements.'

All animals were divided into groups by the randomisation method. The absence of external indications of diseases and homogeneity over the body weight were considered as criteria of appropriate randomisation. The operation with laboratory animals was performed according to the Guiding Principles for Biomedical Research Involving Animals (Geneva, 1985), the Helsinki Declaration on the Human Attitude to Animals (Helsinki, 2000), the European Convention for the Protection of Vertebrate Animals Used for Experimental and Other Scientific Purposes (Strasbourg, 1986), and the Rules for Laboratory Practice (order no. 708 n of the Ministry of Health Protection and Social Development of the Russian Federation of 23 August 2010).

3 Results and discussion

3.1 Synthesis and characterisation of nanocomposites

The nanocomposites Se^0/κ-CG with selenium content 0.3, 0.6, 1, 1.5, and 3.0% were synthesised by oxidation of Se^{2-} to Se^0 in the water solution of κ-CG. Se^{2-} ions were generated previously by the reduction of elemental bulk-selenium with hydrazine hydrate in an alkaline medium. As a result, the selenium is dissolved, and highly reactive selenide anions were formed according to (3)

$$2Se + 4NaOH + N_2H_4 \cdot H_2O \rightarrow 2Na_2Se + N_2\uparrow + 5H_2O \qquad (3)$$

The formation of selenium nanoparticles is the result of a multi-stage process of nucleation of a new phase, one stage of which is the sequential coalescence of selenium atoms formed as a result of oxidation by molecular oxygen of Se^{2-} ions with further stabilisation of nanoparticles by κ-CG macromolecules [28, 34]. According to the data of TEM, nanocomposites Se^0/κ-CG are produced in the form of spherical nanoparticles dispersed in the polysaccharide matrix of κ-CG (Fig. 1). Sizes of Se^0NPs vary 3–37 nm. It is found that an increase of the quantitative content of selenium in the nanocomposites from 0.3 to 3.0% augments the average size of the formed Se^0NPs from 4.6 to 24.5 nm, respectively, as well as leads to the broadening of their disperse distribution. The diagrams of the size distribution of particles in the obtained nanocomposites are unimodal. Also, the log-normal type of dispersion distribution shows that the growth and aging of Se^0NPs occur due to the sequential coalescence of selenium atoms and small nanoparticles to large ones, and not due to the massive aggregation of formed nanoparticles.

The size of the largest fraction of forming Se^0NPs ranges 5–7, 7–14, and 16–24 nm for samples with 0.6, 1.5, and 3.0% Se, respectively. The wider disperse distribution of Se^0NPs in the sample with high selenium content is caused by differences in the synthesis conditions of nanocomposites. In particular, due to the fact that the concentration of formed nuclei of a new phase in the reaction medium during the synthesis is theoretically constant, the growth of nanoparticles occurs owing to sorption of the generated selenium atoms on the surface of the nuclei (or growing nanoparticle) [34]. This process is stochastic and is determined by local conditions of the reaction medium (the number of selenium atoms and nuclei, the conformation of stabiliser macromolecules in a unit of volume and at that moment). Consequently, the increase in the concentration of the selenium precursor in the reaction medium is accompanied by the growth of selenium nanoparticles and the broadening of their disperse distribution due to the growth of the formed nuclei. However, the literature contains precedents of both increasing and decreasing the size of nanoparticles with

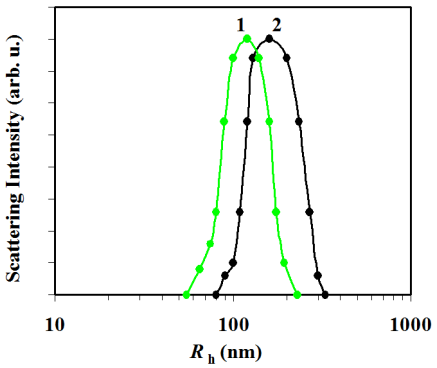

Fig. 2 *R_h-distributions of water-salt solution nanocomposites Se^0NPs/κ-CG containing: (1) 0.3% Se, (2) 1.5% Se*

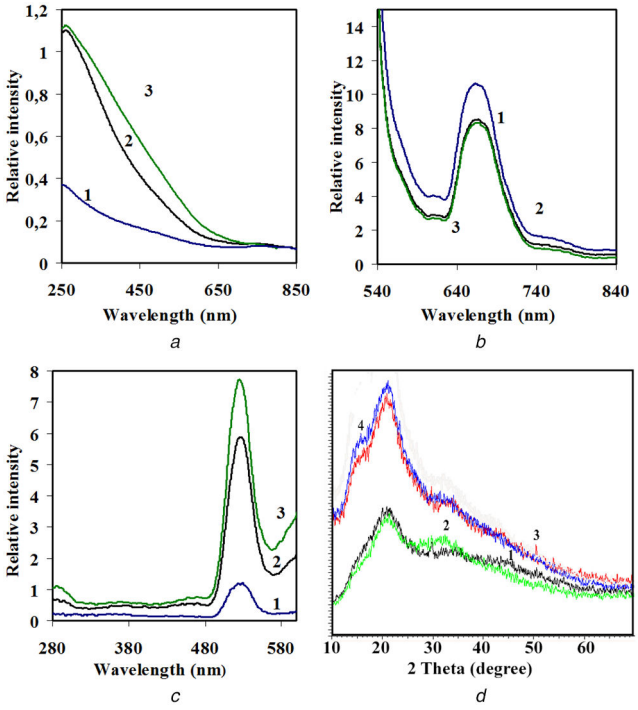

Fig. 3 *Optical and X-ray Characteristics of nanocomposites*

(a) Absorption, ***(b)*** Emission, ***(c)*** Excitation spectra of 0.2% water-solution nanocomposites Se^0/κ-CG containing: (1) 0.3% Se, (2) 1% Se, (3) 1.5% Se; ***(d)*** XRD of (1) native κ-CG, (2) nanocomposites Se^0/κ-CG containing 0.6% Se, (3) 1% Se, (4) 1.5% Se

augmentation of the precursor's concentration [35, 36]. The direction of change in particle size depends on the selected synthetic method and the initial reagents (mainly, the stabiliser). In our case, we employed macromolecules of sulphated polysaccharide κ-CG as a stabiliser, which are present in the reaction medium in excess in comparison with the selenium precursor. As a result, the observed growth of the selenium nanoparticles size and the broadening of their polydispersity may also be due to the changes in diffusion characteristics of the reaction medium upon addition of a large amount of Se^{2-} ions (and consequently Na^+). The polyelectrolyte nature of κ-CG causes the interaction of its macromolecules with Na^+ ions (under conditions of their excess) leading to the structuring of macromolecules in a solution and the loss of part of the diffusion mobility. Eventually, the viscosity of the reaction medium increases and the diffusion of selenium atoms to the surface of growing nuclei and nanoparticles is hampered. This enhances the degree of stochasticity of the nanoparticles formation and broadens their polydispersion. In addition, the increased concentration of Se^{2-} ions in the reaction medium at the same concentration of κ-CG (and, accordingly, the increase of the solution ionic strength) leads to a decrease in the aggregate stability of the obtained nanoparticles and their further uneven growth.

Previously, it was shown in [37, 38] that in the presence of potassium ions the κ-CG macromolecules transform from a state of a ball to a spiral structure. These spirals are grouped together through interaction with the potassium ion to afford a number of macromolecular aggregates, which are also involved in the synthesis of nanocomposites. This leads to a pronounced polydispersity of the obtained nanomaterials and generation of nanoparticles aggregates identified by TEM and DLS. The replacement of potassium hydroxide by sodium hydroxide allows neutralising the ion-mediated aggregation processes in the reaction medium. However, the introduction of large amounts of sodium ions is still accompanied by a partial structuring of κ-CG macromolecules, but to a lesser degree than in the case of potassium ions [39].

The stability and hydrodynamic radius of Se^0NPs-containing nanocomposites have been assessed by ζ-potential and DLS analysis. In the present study, ζ-potential of all nanocomposites varies from −28 to −32 mV. Negative ζ-potential of the initial κ-CG and its Se-containing nanocomposites are originated mainly from negatively charged sulpho-groups of the κ-CG. The obtained values indicate sufficiently pronounced stability of aqueous solutions of the obtained nanocomposites.

The DLS data (Fig. 2) show that the obtained nanocomposites in aqueous solutions represent stable colloidal particles with average size (hydrodynamic radius – R_h) of 120–160 nm in dependence on the synthesis conditions. The increase of the amount of Se^0NPs in the nanocomposite is accompanied by the growth of R_h and widening of the degree of particles polydispersity in solution. This can probably be due to both an increase in the average size of selenium nanoparticles in the course of introduction of higher amounts of the selenium precursor into the reaction medium and the enhancement of the ionic strength of the precursor solution containing, apart from Se^{2-} and Na^+ ions. In the presence of the latter (in high concentrations) a partial aggregation of CG macromolecules occurs, which causes an increase of R_h particles in aqueous solutions of nanocomposites.

The optical properties of the obtained nanocomposites have been investigated by optical spectroscopy in the visible region of the spectrum. The absorption, emission, and excitation spectra have been measured at room temperature. No bands are detected in the absorption spectra of aqueous solutions of the Se^0/κ-CG nanocomposites (Fig. 3). A monotonous rise from the low- to high-energy spectral region and a wide peak at about 260 nm are observed in all absorption spectra (Fig. 3*a*). Also, a lower intensity plateau appears at ∼530 nm. The peak of absorption in the 260 nm region can be attributed to the interband and core electronic transitions, while the plateau in the visible region is probably due to surface plasmon resonance [18]. The excitation spectra of aqueous solutions of nanocomposites are characterised by the presence of several bands of different intensities (Fig. 3*c*).

In accordance with previous studies, the excitation bands in the short wavelength region most likely belong to the κ-CG polysaccharide matrix [21]. The band at 527 nm presumably corresponds to the electron transitions from low to higher energy levels in the Se^0NPs [18]. This is confirmed by the explicit concentration dependence of the excitation band intensity on the content of Se^0NPs in the composite. Luminescence properties of water solutions of Se^0NPs stabilised by κ-CG have been studied. It is found that a band has a peak at about 660 nm (Fig. 3*b*). An increase of the quantitative content of selenium in the nanocomposite from 0.3 to 1.5% is accompanied by a slight shift of the luminescence maximum to a longer wavelength region, as well as a decrease in the intensity and quantum yield of luminescence (Table 1). This effect is due to a higher luminescence intensity of small-sized Se^0NPs, which are the predominant component of nanocomposites with 0.3% Se^0, as well as by the concentration factor of luminescence quenching.

By X-ray diffraction analysis, it has been established that all obtained Se^0/κ-CG nanocomposites are X-ray amorphous

substances. Their diffraction pattern follows the X-ray patterns of the native polysaccharide matrix of κ-CG (Fig. 3*d*).

The available free radicals DPPH$^{\bullet}$ and cation-radical ABTS$^{+\bullet}$ have been employed to evaluate the total antiradical activity of the resulting Se^0-containing nanocomposites. These radicals are very often used as test systems to quantify the antioxidant activity of the studied objects. As a control, aqueous solutions of a known antioxidant, ascorbic acid, as well as the initial polysaccharide κ-CG have been used. The study of the damaging effect of the synthesised nanocomposites on the free radical of DPPH$^{\bullet}$ reveals that the initial κ-CG in the concentration of 0.25–9.3 mg/ml almost does not have an inhibitory effect (Fig. 4*a*). The anti-radical activity of κ-CG against DPPH$^{\bullet}$ does not exceed 1.9%. This enables us to conclude that κ-CG is a substance with extremely low anti-radical activity. In contrast, Se^0/κ-CG nanocomposites in the same concentrations show a strong antiradical effect (up to 50%). The increase in the quantitative content of Se^{0}NPs in nanocomposites from 0.3 to 1.5% is accompanied by a decrease of the inhibitory concentration value (IC) $IC_{DPPH^{\cdot}}$ from 9.3 to 5.2 mg/ml, thus confirming direct participation of Se^0 in DPPH$^{\bullet}$ inhibition reactions.

The anti-radical activity of the ascorbic acid, used as a standard, in the same concentrations is higher and reaches 95.4–96.7%. Considering the effect of selenium on the antioxidant activity of nanocomposites and low content of selenium in the nanocomposites (0.3–1.5%), as well as the total ratio of moles of the substrate and free radical DPPH$^{\bullet}$, it can be assumed that the found values of antioxidant activity of the obtained nanocomposites are comparable with those of the well-known antioxidant, ascorbic acid.

Table 1 Dimensional and luminescent parameters for Se/κ-CG nanocomposites

% Se^0	Average size of the particle (the date of TEM), nm	Average quantum yield	Maximum wavelength luminescence, nm
0.3%	4.6	0.047 ± 0.005	663.5
1%	8.2	0.028 ± 0.002	665.5
1.5%	11.0	0.026 ± 0.004	666.5

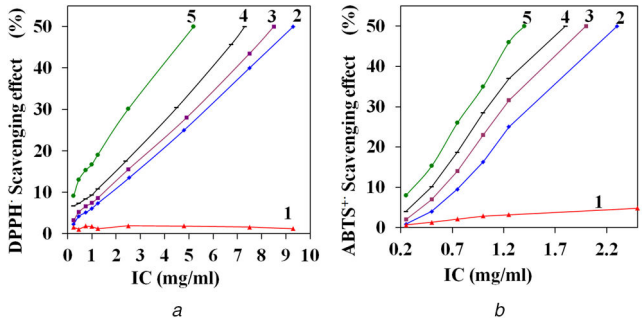

Fig. 4 *Concentration dependence of the value of antioxidant activity against*

(a) DPPH$^{\bullet}$, ***(b)*** ABTS$^{+\bullet}$ of (1) the initial κ-CG, (2) Se^0-containing nanocomposites: 0.3% Se, (3) 0.6% Se, (4) 1% Se, (5) 1.5% Se

So, it is found that for 50% neutralisation of 3.2×10^{-7} mole of the DPPH$^{\bullet}$ 8.8×10^{-7}–2.4×10^{-6} mole of Se^0 is sufficient. These data correlate well with $IC_{50\%}$ for ascorbic acid (2.4×10^{-6} mole) (Table 2).

As follows from Table 2, the increase in the average size of Se^{0}NPs is accompanied by a slight growth of selenium moles, which are needed to achieve 50% neutralisation of DPPH$^{\bullet}$. Most likely, this pattern is due to the less pronounced antioxidant activity in larger nanoparticles present in samples with increased selenium content in their composition. Previously, information about the effect of nanoparticle size on their biological properties (size effect) has been reported [40] data obtained in the present work confirms once again the findings of the determining influence of nanoparticles size on their properties (including biological ones).

The free cation-radical ABTS$^{+\bullet}$ is more reactive than DPPH$^{\bullet}$ and much more sensitive to potential antioxidants. Respectively, the concentration of aqueous solutions of selenium nanocomposites is significantly lower than for DPPH$^{\bullet}$ when inhibition of 50% of the ABTS$^{+\bullet}$ is observed. It is found that the initial κ-CG solution (taken for comparison) has a weak inhibitory effect on ABTS$^{+\bullet}$, the value of antioxidant activity being 4.8% at the highest concentrations. This confirms the low antioxidant activity of the polysaccharide matrix, whereas Se^0-containing κ-CG-derived nanocomposites exhibit a strong antioxidant effect on ABTS$^{+\bullet}$. An increase in the quantitative content of selenium in the nanocomposites from 0.3 to 1.5% decreases the $IC_{50\%}$ $ABTS^{+\cdot}$ value from 2.3 to 1.4 mg/ml (Fig. 4*b*). These data once again evidence the key role of Se^{0}NPs in the antioxidant activity of nanocomposites.

We have also employed ascorbic acid solutions in concentrations similar to those of aqueous solutions of the tested nanocomposites as control. The ascorbic acid shows higher activity (up to 98%) than nanocomposites in experiments with ABTS$^{+\bullet}$. However, the calculations have allowed establishing the molar ratio between the antioxidant tested and ABTS$^{+\bullet}$. It is found that 50% neutralisation of 1.5×10^{-7} mol of the ABTS$^{+\bullet}$ requires 8.9×10^{-8}–2.6×10^{-7} mol of the Se^0. The obtained values are well correlated with an amount of moles of the ascorbic acid (5.1×10^{-7}) that are necessary for 50% neutralisation of the ABTS$^{+\bullet}$ (Table 3).

This confirms the pronounced antioxidant effect of the obtained nanocomposites. Like in the case of $DPPH^{\cdot}$, an increase in the nanoparticles' size is accompanied by the growth of Se^0 amount required for $ABTS^{+\cdot}$ neutralisation from 8.9×10^{-8} to 2.6×10^{-7} moles, and, respectively, by a decrease in antioxidant activity of the nanocomposites.

It can be assumed that the anti-radical activity of the nanocomposites is based on the known high chemical reactivity of selenium, which can participate in a number of reactions, including redox ones. The inhibition of the model-free radicals DPPH and ABTS is promoted either by the proton transfer reaction (if ascorbic acid is used as an antioxidant) or by single-electron transfer. The latter is most probable when selenium nanocomposite is employed for inhibition of these radicals [41].

According to the literature data, the surface of selenium nanoparticles, even in the presence of the stabilising agent, contains uncompensated atom-ionic selenium states, which can

Table 2 Quantitative and dimensional characteristics of the Se^0/κ-CG nanocomposites at 50% $IC_{DPPH^{\cdot}}$ value as compared with ascorbic acid

% Se^0	Particle size, nm	Specific surface area m^2/kg	*C*, mg/ml	Mass of Se, mg	mol Se^0 (AA)	Mol DPPH	AOA, %
0.3	4.6	3×10^5	9.3	0.07	8.8×10^{-7}	3.2×10^{-7}	50.0
0.6	6.8	2.0×10^5	8.5	0.13	1.6×10^{-6}	3.2×10^{-7}	50.0
1	8.2	1.7×10^5	7.1	0.18	2.2×10^{-6}	3.2×10^{-7}	50.0
1.5	11.0	12.6×10^4	5.2	0.19	2.4×10^{-6}	3.2×10^{-7}	50.0
ascorbic acid (AA)			0.17	—	2.4×10^{-6}	3.2×10^{-7}	50.0

Table 3 Quantitative and dimensional characteristics of the Se^0/κ-CG nanocomposites at 50% IC_{ABTS} value as compared with ascorbic acid

% Se^0	Particle size, nm	Specific surface area m^2/kg	*C*, mg /ml	Mass of Se, mg	mol Se^0 (AA)	mol ABTS	AOA, %
0.3	4.6	3×10^5	2.3	0.007	8.9×10^{-8}	1.5×10^{-7}	50.0
0.6	6.8	2.0×10^5	2.0	0.012	1.5×10^{-7}	1.5×10^{-7}	50.0
1	8.2	1.7×10^5	1.8	0.018	2.3×10^{-7}	1.5×10^{-7}	50.0
1.5	11.0	12.6×10^4	1.4	0.021	2.6×10^{-7}	1.5×10^{-7}	50.0
ascorbic acid (AA)			0.09	—	5.1×10^{-7}	1.5×10^{-7}	50.0

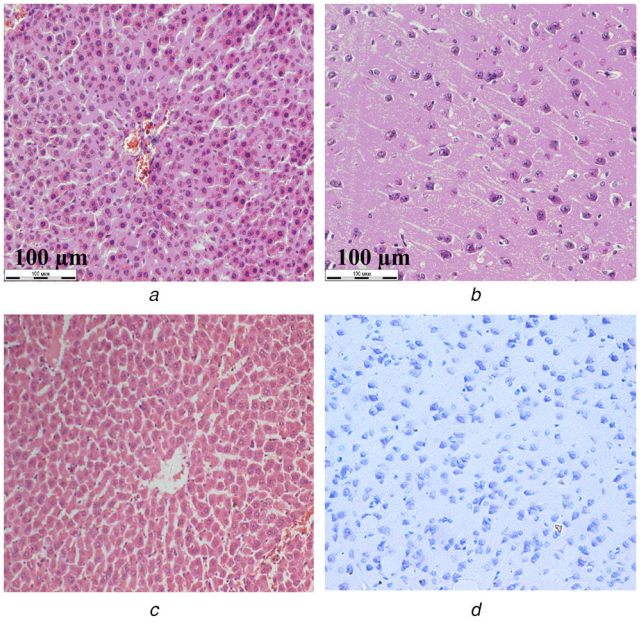

Fig. 5 *Histological slides of*
(a, c) Liver, ***(b, d)*** Brain of rats in the control (upper row) and experimental (lower row) groups administrated 6.8 nm Se^0NPs

interact with both polar functional groups of the stabiliser molecules and with other substances contained in their medium [42]. Probably, in this case, these vacant ionic and, likely, unpaired selenium states on the nanoparticles' surface are involved in the single-electron transfer reactions. As a result, DPPH and ABTS lose their primary radical structure and the test solution (used for detection of inhibition) changes its colour. Owing to the fact that these uncompensated states are located exclusively on the surface of the nanoparticle (interface), the surface area of the nanoparticles exerts the determining effect on the anti-radical activity of selenium nanoparticles.

The increase in the nanoparticles' size from 4.6 to 11.0 nm is accompanied by a decrease in the minimum inhibitory concentration of the nanocomposites required to neutralise 50% of free radical due to the total augmentation of the selenium nanoparticles concentration in the nanocomposites. However, recalculation of selenium moles required for this neutralisation reveals that radical inhibition requires a higher amount of selenium moles. Given the determinant role of the surface area of selenium nanoparticles, it can be assumed that the growth of nanoparticles is accompanied by a slight decrease in their surface area (Tables 2 and 3). Consequently, the number of uncompensated ionic and unpaired selenium states, capable of interacting with DPPH and ABTS, also diminishes. Probably, these factors slightly decrease antioxidant activity. The obtained data are in good agreement with other works and confirm the size dependence of the antiradical activity of the selenium nanoparticles.

The experimental evaluation of the toxicity of the obtained nanocomposites bearing selenium particles of different size reveals no statistically significant abnormalities from the control in the behaviour of animals and their appearance. After administration of the maximum dose (2000 mg/kg) of the studied nanocomposites to animals, as well as during 14 days of observation, all species remained neat, their reactions to stimuli did not change, and hyper salivation was also not observed. Decapitation of the animals and their macroscopic examination showed no changes in the structure of their main internal organs and systems. In particular, the thoracic and abdominal cavities contained no exudate and adhesions. The position of the organs was normal. No changes in the size or shape of the heart were observed, intima of the vessels and blood supply were normal. The lumen of the trachea and bronchi was satisfactory; there was no narrowing or obstruction. Lungs were of natural colour and size with a uniform pale pink surface. The thyroid gland had a normal size with moderately dense consistency. The oesophagus also showed visible narrowing or obstruction; the mucous membrane of the oesophagus was smooth and glitter. The stomach was of normal size and colour. Food was evacuated from the stomach with a normal rate. The intestine was of common colour with clearly visible peristalsis. The liver had normal size, colour, and consistency; its blood supply was moderate. The pancreas was of natural size, colour, and consistency. The size, colour, and density of the spleen were also within normal range. The kidneys were of normal size and brown. The cortex and medulla of the organ were clearly distinguishable in the section. The adrenal glands were round, white, and moderately dense. The urinary bladder was of common size, the evacuation of urine was normal; the mucous membrane of the organ was smooth and glitter. The colour and shape of the testicles were normal. The membranes of the brain were glitter, thin and smooth. Ventricular dilatation in the frontal section was not observed. There were no visible changes in the internal organs and glands. Thus, taking into account the set of indicators and the absence (during the observation period) of animal deaths, the studied nanocomposites with selenium particle sizes of 6.8 and 24.5 nm have been assigned to hazard class 5 and are low-hazard substances.

The study of the biological effect of selenium nanoparticles with an average size of 6.8 and 24.5 nm, as well as their biodistribution has shown that the state of rat organs after 10-day administration of selenium nanocomposites and pure κ-CG nanocomposites did not differ from that of the control group. The macroscopic picture of the main organs and systems of the organism was within the normal range. The results obtained are in good agreement with the experimental data on the toxicity of selenium nanocomposites and indicate low toxicity of these compounds. Microscopic examination of the liver, kidneys, and brain of rats treated with nanocomposites and the original κ-CG revealed that the structure of these organs also did not have statistically significant abnormalities from the control. Fig. 5 shows histological samples of liver and brain of rats in the control and experimental groups. The liver sections of experimental animals of all groups were characterised by the normal blood supply to sinusoidal capillaries, central veins, and portal tracts. The latter were not expanded, without signs of sclerosis and inflammation. The beam-radiary structure of the hepatic acinus is preserved. The number of Kupffer's star macrophages had no statistically significant differences ($p = 0.4$) from the control indicators: 123.0–173.0 in the experimental groups and 145.0–177.0 in the control group. The sections of kidneys revealed normal blood supply to the cortex and medulla. The state of the renal artery wall and arterioles is normal. The interstitial space is satisfactory. The structure of renal glomeruli is preserved. The area of the Shumlyansky–Bowman capsule did not have a statistically significant difference ($p = 0.1$–0.7) from the control indicators: 35,422.6–36,167.7 μm^2 in

Table 4 Values various cell populations in brain tissue per unit area (0.2 mm^2)

Group	A number of neurons per unit area (un.)	A number of astroglial cells per unit area (un.)	A number of degenerated neurons per unit area (un.)	A number of neuronophagia acts per unit area (un.)
control	358.5 (342.0–375.5)	336.5 (319.0–364.5)	4.0 (2.0–4.5)	2.5 (0.5–4.5)
Se^0NPs (6.8 nm)	315.5 (301.5–334.5)	278.5[a] (269.0–292.0)	5.5 (3.5–7.0)	2.5 (2.0–4.0)
Se^0NPs (24.5 nm)	385.0 (378.5–392.5)	357.0 (325.5–385.0)	6.0 (5.0–7.0)	3.5 (2.0–4.0)
κ-CG	360.0 (339.0–371.5)	314.0 (298.0–329.5)	3.0 (1.0–4.5)	2.5 (1.5–4.0)

[a]The indicator differs from the control values.

Table 5 Selenium concentration in organs of rat (in parentheses is the standard deviation)

Organ	Selenium concentration, μg/g		
	Control group	First group (6.8 nm Se^0NPs)	Second group (24.5 nm Se^0NPs)
liver	0.079 ± 0.005 (0.012)	0.210 ± 0.016 (0.036)	0.096 ± 0.006 (0.013)
kidney	0.035 ± 0.003 (0.006)	0.151 ± 0.002 (0.006)	0.036 ± 0.002 (0.004)
brain	0.030 ± 0.002 (0.004)	0.061 ± 0.003 (0.007)	0.027 ± 0.004 (0.001)

the experimental groups and 36,204.8 (30,303.4–39,741.2) μm^2 in the control group. No foci of inflammation or necrosis of the renal tissue were observed. The epithelium of the distal and proximal renal tubules was normal.

An exception is the brain of rats from the group treated with a nanocomposite having small particle size (6.8 nm). In this group, a statistically significant ($p = 0.03$) decrease of astroglial cells was observed as compared to the control group. The results of the microscopic examination of rat brain sections are shown in Table 4.

In addition, it was found that if rats were administrated with the nanocomposite having small particle size, the level of selenium concentration was increased in liver, kidneys, and brain compared to the control group and the group treated with the nanocomposite having a particle size of 24.5 nm (Table 5).

Probably, due to high chemical and biological activity, small-sized selenium nanoparticles are more intensively involved in biochemical interactions with organic compounds, including the substitution of sulphur in sulphur-containing proteins, participate in the synthesis of specific selenoproteins, and also form a renewable supply of selenium in the organism. These facts explain the increase in the selenium concentration in the tissues of animals treated with nanoparticles of 6.8 nm in size. On the contrary, significantly larger particles (24.5 nm), likely due to their low reactivity, are partially eliminated from the organism through natural mechanisms of enzymatic reduction to hydrogen selenide, as well as reverse enzymatic methylation to sequentially afford methylhydroselenide (Se-containing analogue of methanol), dimethylselenide and trimethylselenonium cation. These Se compounds are excreted with urine, and dimethylselenide is eliminated in large amounts with sweat as well [43–45].

In addition, the observed significant increase of selenium concentration in the brain results from the penetration of small selenium nanoparticles through the blood–brain barrier, which still remains impermeable to large particles. At the same time, a decrease in the number of astroglial cells is probably due to the effect of selenium nanoparticles on the astroglial elements of the sensorimotor cortex. Given the high importance of astrocytes in maintaining of brain tissue homoeostasis, such selectivity can lead to essential changes in the functional state of the sensorimotor cortex in the long-term post-contact period. The revealed cell selectivity of the studied nanocomposite with a selenium nanoparticle size of 6.8 nm requires further detailed study.

4 Conclusion

In this study, a newly available and environmentally friendly method for the synthesis of water-soluble selenium nanoparticles stabilised by the κ-CG shell has been developed. The potential anti-radical and luminescent activity of the nanocomposites is studied. The structure of Se^0NPs is confirmed by TEM, DLS, XRD, PL, and optical spectroscopy. It is found that the obtained nanocomposites have a pronounced luminescence, the main parameters of which (quantum yield and excitation–emission range) depend on the size of selenium nanoparticles. With the use of model-free radicals ABTS and DPPH, it is established that the nanocomposites have high anti-radical activity, the value of which is inversely related to the size of nanoparticles and is determined exclusively by selenium nanoparticles incorporated in the polysaccharide. In vivo testing of the biological effect of the obtained nanocomposites made it possible to establish and confirm the determining effect of the size of nanoparticles on their properties, in particular, pronounced accumulation of selenium in the body with an experimentally recorded decrease in astroglial cells when administering small nanoparticles and the absence of any effects of accumulation and biological effects of large nanoparticles. Also, we found low toxicity of all obtained nanocomposites. Together, this determines the prospects for further research of the obtained nanomaterials for the development of modern non-toxic biocompatible materials for design visualising and therapeutic agents for biomedical applications.

5 Acknowledgments

This work was supported by the Russian Science Foundation (grant no. 18-75-00080) – synthesis of selenium-containing nanocomposites and study of their structure and antiradical activity, and within the framework of the state task of A.E. Favorsky Irkutsk Institute of Chemistry of SB RAS (IrICh SB RAS) (project no. AAAA-A19-119022690046-4 – DLS-characterisation of nanocomposites). The authors wish to thank the Isotopegeochemical research center for Collective Use (A.P. Vinogradov Institute of Geochemistry of the Siberian Branch of the Russian Academy of Sciences) and the Baikal Analytical Centre (Irkutsk Institute of Chemistry of the Siberian Branch of the Russian Academy of Sciences) for providing equipment.

6 References

[1] Guan, B., Yan, R., Li, R., *et al.*: 'Selenium as a pleiotropic agent for medical discovery and drug delivery', *Int. J. Nanomed.*, 2018, **13**, pp. 7473–7490, doi: 10.2147/IJN.S181343

[2] Hosnedlova, B., Kepinska, M., Skalickova, S., *et al.*: 'Nano-selenium and its nanomedicine applications: a critical review', *Int. J. Nanomed.*, 2018, **13**, pp. 2107–2128, doi: 10.2147/IJN.S157541

[3] Barciela, J., Herrero Latorre, C., Garcia-Martín, S., *et al.*: 'A brief study of the role of selenium as antioxidant', *Electron. J. Environ. Agric. Food Chem.*, 2008, **7**, pp. 3151–3155

[4] Mangiapane, E., Pessione, A., Pessione, E.: 'Selenium and selenoproteins: an overview on different biological systems', *Curr. Protein Pept. Sci.*, 2014, **15**, pp. 598–607, doi: 10.2174/1389203715666140608151134

[5] Hu, C.H., Li, Y.L., Xiong, L., *et al.*: 'Comparative effects of nano elemental selenium and sodium selenite on selenium retention in broiler chickens', *Anim. Feed Sci. Technol.*, 2012, **177**, pp. 204–210, doi: 10.1016/j.anifeedsci.2012.08.010

[6] Aruxandei, D.C., Frincu, R.M., Capra, L., *et al.*: 'Selenium analysis and speciation in dietary supplements based on next-generation selenium ingredients', *Nutrients*, 2018, **10**, pp. 1466–1500, doi: 10.3390/nu10101466

[7] Fang, X., Li, C., Zheng, L., *et al.*: 'Dual-targeted selenium nanoparticles for synergistic photothermal therapy and chemotherapy of tumors', *Chem. - Asian J.*, 2018, **13**, pp. 996–1004, doi: 10.1002/asia.201800048

[8] Tan, H.W., Mo, H.Y., Lau, A.T.Y., *et al.*: 'Selenium Species: current Status and potentials in cancer prevention and therapy', *Int. J. Mol. Sci.*, 2018, **20**, pp. 75–101, doi: 0.3390/ijms20010075

[9] Wang, Y., Chen, P., Zhao, G., *et al.*: 'Inverse relationship between elemental selenium nanoparticle size and inhibition of cancer cell growth in vitro and in vivo', *Nanotoxicol. Nanomed.*, 2015, **85**, pp. 71–77

[10] Khurana, A., Tekula, S., Saifi, M.A., *et al.*: 'Therapeutic applications of selenium nanoparticles', *Biomed. Pharmacother.*, 2019, **111**, pp. 802–812, doi: 10.1016/j.biopha.2018.12.146

[11] Amini, S.M., Mahabadi, V.P.: 'Selenium nanoparticles role in organ systems functionality and disorder', *Nanomed. Res. J.*, 2018, **3**, pp. 117–124, doi: 10.22034/NMRJ.2018.03.001

[12] Maiyo, F., Singh, M.: 'Selenium nanoparticles: potential in cancer gene and drug delivery', *Nanomedicine*, 2017, **12**, pp. 1075–1089, doi: 10.2217/nnm-2017-0024

[13] Zhanga, J., Tenga, Z., Yuanb, Y., *et al.*: 'Development, physicochemical characterization and cytotoxicity of selenium nanoparticles stabilized by beta-lactoglobulin', *Int. J. Biol. Macromol.*, 2018, **107**, pp. 1406–1413, doi: 10.1016/j.ijbiomac.2017.09.117

[14] Yan, J.K., Qiu, W.Y., Wang, Y.Y., *et al.*: 'Fabrication and stabilization of biocompatible selenium nanoparticles by carboxylic curdlans with various molecular properties', *Carbohydr. Polym.*, 2018, **179**, pp. 19–27, doi: 10.1016/j.carbpol.2017.09.063

[15] Zhang, S.Y., Zhang, J., Wang, H.Y., *et al.*: 'Synthesis of selenium nanoparticles in the presence of polysaccharides', *Mater. Lett.*, 2004, **58**, pp. 2590–2594, doi: 10.1016/j.matlet.2004.03.031

[16] Vyas, J., Rana, S.: 'Antioxidant activity and green synthesis of selenium nanoparticles using allium sativum extract', *Int. J. Phytomed.*, 2017, **9**, pp. 634–641, doi: 10.5138/09750185.2185

[17] Quoc, N., Phan, H., Tuanb, D., *et al.*: 'Gamma Co-60 ray irradiation synthesis of dextran stabilized selenium nanoparticles and their antioxidant activity', *Mater. Chem. Phys.*, 2018, **205**, pp. 29–34, doi: 10.1016/j.matchemphys.2017.11.003

[18] Singh, S.C., Mishra, S.K., Srivastava, R.K., *et al.*: 'Optical properties of selenium quantum dots produced with Laser irradiation of water suspended Se nanoparticles', *J. Phys. Chem. C*, 2010, **114**, pp. 17374–17384, doi: 10.1021/jp105037w

[19] Lesnichaya, M.V., Aleksandrova, G.P., Feoktistova, L.P., *et al.*: 'Silver-containing nanocomposites based on galactomannan and carrageenan: synthesis, structure, and antimicrobial properties', *Russ. Chem. Bull.*, 2010, **59**, pp. 2323–2328, doi: 10.1007/s11172-010-0395-6

[20] Lesnichaya, M.V., Sukhov, B.G., Aleksandrova, G.P., *et al.*: 'Chiroplasmonic magnetic gold nanocomposites produced by one-step aqueous method using κ-carrageenan', *Carbohydr. Polym.*, 2017, **175**, pp. 18–26, doi: 10.1016/j.carbpol.2017.07.040

[21] Lesnichaya, M.V., Shendrik, R.Y., Sapozhnikov, A.N., *et al.*: 'Synthesis and luminescent properties of water-soluble nanobiocomposite CdSe/polysaccharide quantum dots', *Russ. Chem. Bull.*, 2017, **66**, pp. 2321–2326, doi: 10.1007/s11172-017-2023-1

[22] Lesnichaya, M.V., Sukhov, B.G., Sapozhnikov, A.N., *et al.*: 'New nanobiocomposites of ammonium magnesium phosphate and carrageenan as efficient prebiotics', *Dokl. Chem.*, 2017, **457**, pp. 144–147, doi: 10.1134/S0012500814080023

[23] Ruocco, N., Costantini, S., Guariniello, S., *et al.*: 'Polysaccharides from the marine environment with pharmacological, cosmeceutical and nutraceutical potential', *Molecules*, 2016, **21**, p. 551, doi: 10.3390/molecules21050551

[24] Sebaaly, C., Karaki, N., Chahine, N., *et al.*: 'Polysaccharides of the red algae pterocladia growing on the Lebanese coast: isolation, structural features with antioxidant and anticoagulant activities', *J. Appl. Pharm. Sci.*, 2012, **2**, pp. 1–10, doi: 10.7324/JAPS.2012.21001

[25] Suganya, A.M., Sanjivkumar, M., Chandran, M.N., *et al.*: 'Pharmacological importance of sulphated polysaccharide carrageenan from red seaweed kappaphycus alvarezii in comparison with commercial carrageenan', *Biomed. Pharmacother.*, 2016, **84**, pp. 1300–1312, doi: 10.1016/j.biopha.2016.10.067

[26] Sudha, P.N.: '*Industrial applications of marine biopolymers*' (CRC Press, USA, 2017), p. 626

[27] Pangestuti, R., Kim, S.K.: 'Biological activities of carrageenan', *Adv. Food Nutr. Res.*, 2014, **72**, pp. 113–124, doi: 10.1016/B978-0-12-800269-8.00007-5

[28] Lesnichaya, M.V., Shendrik, R.Y., Sukhov, B.G.: 'Relation between excitation dependent luminescence and particle size distributions for the selenium nanoparticles in κ-carrageenan shell', *J. Lumin.*, 2019, **211**, pp. 305–313, doi: 10.1016/j.jlumin.2019.03.056

[29] Yamaguchi, T., Takamura, H., Matoba, T., *et al.*: 'HPLC method for evaluation of the free radical-scavenging activity of foods by using 1,1-diphenyl-2-picrylhydrazyl', *Biosci. Biotechnol. Biochem.*, 1998, **62**, pp. 1201–1204, doi: 10.1271/bbb.62.1201

[30] Molyneux, P.: 'The use of the stable free radical diphenylpicrylhydrazyl (DPPH) for estimating antioxidant activity', *Songkl. J. Sci. Technol.*, 2004, **26**, pp. 211–219

[31] Cai, W., Hu, T., Bakry, A.M., *et al.*: 'Effect of ultrasound on size, morphology, stability and antioxidant activity of selenium nanoparticles dispersed by a hyperbranched polysaccharide from Lignosus rhinocerotis', *Ultrason. Sonochem.*, 2018, **42**, pp. 823–831, doi: 10.1016/j.ultsonch.2017.12.022

[32] Re, R., Pellegrini, N., Proteggente, A., *et al.*: 'Antioxidant activity applying an improved ABTS radical cation decolorization assay', *Free Radicals Biol. Med.*, 1999, **26**, pp. 1231–1237

[33] Erel, O.: 'A novel automated direct measurement method for total antioxidant capacity using a new generation, more stable ABTS radical cation', *Clin. Biochem.*, 2004, **37**, pp. 277–285, doi: 10.1016/j.clinbiochem.2003.11.015

[34] Thanh, N.T., Maclean, N., Mahiddine, S.: 'Mechanisms of nucleation and growth of nanoparticles in solution', *Chem. Rev.*, 2014, **114**, pp. 7610–7630, doi: 10.1021/cr400544s

[35] Dehsari, H.S., Ribeiro, A.H., Ersöz, B., *et al.*: 'Effect of precursor concentration on size evolution of iron oxide nanoparticles', *CrystEngComm*, 2017, **19**, pp. 694–6702, doi: 10.1039/C7CE01406F

[36] Pholnak, C.H., Sirisathitkul, C.H., Suwanboon, S., *et al.*: 'Effects of precursor concentration and reaction time on sonochemically synthesized ZnO nanoparticles', *Mater. Res.*, 2014, **17**, pp. 405–411, doi: 10.1590/S1516-14392013005000192

[37] Gasilova, E.R., Aleksandrova, G.P., Vlasova, E.N., *et al.*: 'Association of κ-carrageenan subjected to deep alkaline hydrolysis', *Biopolymers*, 2018, **109**, p. e23236

[38] Yuryev, V.P., Blumenfeld, A.L., Braudo, E.E., *et al.*: 'Interaction of sodium and potassium ions with κ-carrageenan', *Colloid Polym. Sci.*, 1991, **269**, pp. 850–854, doi: 10.1007/BF00657452

[39] Mangionea, M.R., Giacomazza, D., Bulonea, D., *et al.*: 'K^+ and Na^+ effects on the gelation properties of κ-carrageenan', *Biophys. Chem.*, 2005, **113**, pp. 129–135, doi: 10.1016/j.bpc.2004.08.005

[40] Torres, S.K., Campos, V.L., Leon, C.G., *et al.*: 'Biosynthesis of selenium nanoparticles by Pantoea agglomerans and their antioxidant activity', *J. Nanopart. Res.*, 2012, **14**, pp. 1236–1245, doi: 10.1007/s11051-012-1236-3

[41] Santos-Sanchez, N.F., Salas-Coronado, R., Villanueva-Canongo, C., *et al.*: 'Antioxidant compounds and their antioxidant mechanism', in Shalaby, E. (Ed.): '*Antioxidants*' (IntechOpen, London, UK, 2019), doi: 10.5772/intechopen.85270, Available from: https://www.intechopen.com/books/antioxidants/antioxidant-compounds-and-their-antioxidant-mechanism

[42] Lujie, L., Zhiping, X., Shuai, N., *et al.*: 'Preparation, characteristics and feeble induced-apoptosis performance of non-dialysis requiring selenium nanoparticles-chitosan', *Mater. Des.*, 2019, **182**, p. 108024, doi: 10.1016/j.matdes.2019.108024

[43] Reich, H.J., Honda, R.J.: 'Why nature chose selenium', *ACS Chem. Biol.*, 2016, **11**, pp. 821–841, doi: 10.1021/acschembio.6b00031

[44] Sayato, Y., Nakamuro, K., Hasegawa, T.: 'Selenium methylation and toxicity mechanism of selenocystine', *Yakugaku Zasshi*, 1997, **117**, (10/11), pp. 665–672

[45] Sunde, R.A.: 'Molecular biology of selenoproteins', *Annu. Rev. Nutr.*, 1990, **10**, pp. 451–474